

## Magnets for the UEM instrument

X. Yang

September 2021

Photon Sciences

**Brookhaven National Laboratory**

**U.S. Department of Energy**

USDOE Office of Science (SC), Basic Energy Sciences (BES) (SC-22)

Notice: This technical note has been authored by employees of Brookhaven Science Associates, LLC under Contract No. DE-SC0012704 with the U.S. Department of Energy. The publisher by accepting the technical note for publication acknowledges that the United States Government retains a non-exclusive, paid-up, irrevocable, world-wide license to publish or reproduce the published form of this technical note, or allow others to do so, for United States Government purposes.

## **DISCLAIMER**

This report was prepared as an account of work sponsored by an agency of the United States Government. Neither the United States Government nor any agency thereof, nor any of their employees, nor any of their contractors, subcontractors, or their employees, makes any warranty, express or implied, or assumes any legal liability or responsibility for the accuracy, completeness, or any third party's use or the results of such use of any information, apparatus, product, or process disclosed, or represents that its use would not infringe privately owned rights. Reference herein to any specific commercial product, process, or service by trade name, trademark, manufacturer, or otherwise, does not necessarily constitute or imply its endorsement, recommendation, or favoring by the United States Government or any agency thereof or its contractors or subcontractors. The views and opinions of authors expressed herein do not necessarily state or reflect those of the United States Government or any agency thereof.

<b>NSLS II TECHNICAL NOTE</b> BROOKHAVEN NATIONAL LABORATORY	NUMBER <b>NSLSII-ASD-TN-371</b>
AUTHOR <b>X. Yang, C. Spataro, L. Doom, F. Lincoln, V. Smaluk, T. Shaftan</b>	DATE <b>09/30/2021</b>
TITLE <b>Magnets for the UEM instrument</b>	

## Abstract

For the magnet system of the UEM instrument, magnetic field specifications are driven by the performance requirements. The ultimate resolution of the UEM depends on how well we can optimize the design of beam focusing magnets via minimizing the spherical and chromatic aberrations. Then, to guarantee the targeted resolution, the tolerances of manufacture and field measurement must be specified via the start-to-end simulation. Then, a magnetic measurement capability is crucial to ensuring the field quality of those magnets. Besides, the magnets should be properly positioned in the UEM beamline to meet those stringent alignment requirements and to take advantage of modern alignment techniques. This note will summarize all those important issues in the frameworks of the BNL UEM LDRD project.

## Introduction

In frameworks of the BNL UEM LDRD project [1, 2], a compact magnetic lens system has been designed as part of the MeV UEM instrument for both single- and multiple-shot imaging modes with 1 nm resolution. To achieve this ambitious design goal, the magnet tolerances for fabrication, measurement, and alignment, must be thoroughly studied via the start-to-end simulation. Also, the lens system is required to have the 5% tunability and to be able to correct the manufacturing error up to  $\pm 2\%$  of the relative gradient error  $\Delta B'/B'$ . To meet all those specifications, we have designed a robust round imaging lens based on quadrupole quintuplet [3] for the Objective, Projector 1, and Projector 2 lenses. Especially, we make the gradient difference small with a total number of three different gradients. Here, two gradients are used to fulfill the round-lens conditions, and one is used to minimize the focal length  $f$ . Minimizing the field interference between the magnets sets the aspect ratio, defined as the ratio of the magnet length and diameter, to 1.5. A 3-stage lens system is required for a total magnification of  $M = 2000$ , with the magnification of each stage of 10, 10, and 20, respectively. The advantage of having a larger magnification for the last stage is to have the same apertures for all magnets. As the result, the resolution is optimized via minimizing the focal length and reducing spherical and chromatic aberrations. The optimized design parameters of the lens magnet are listed in Table I. The longitudinal field profile of the UEM lens is shown in Fig. 1.

UEM lens parameters	K (T/m)	Drift (mm)	Length (mm)	Aperture in diameter(mm)
Quadrupole (1)	<b>-8.7474</b>		12.7	8.4
Quadrupole (2)	<b>31.7710</b>	10.0	12.7	8.4
Quadrupole (3)	<b>-43.8359</b>	10.0	12.7	8.4
Quadrupole (4)	<b>31.7710</b>	10.0	12.7	8.4
Quadrupole (5)	<b>-8.7475</b>	10.0	12.7	8.4

Table I Design parameters of the UEM Lens.

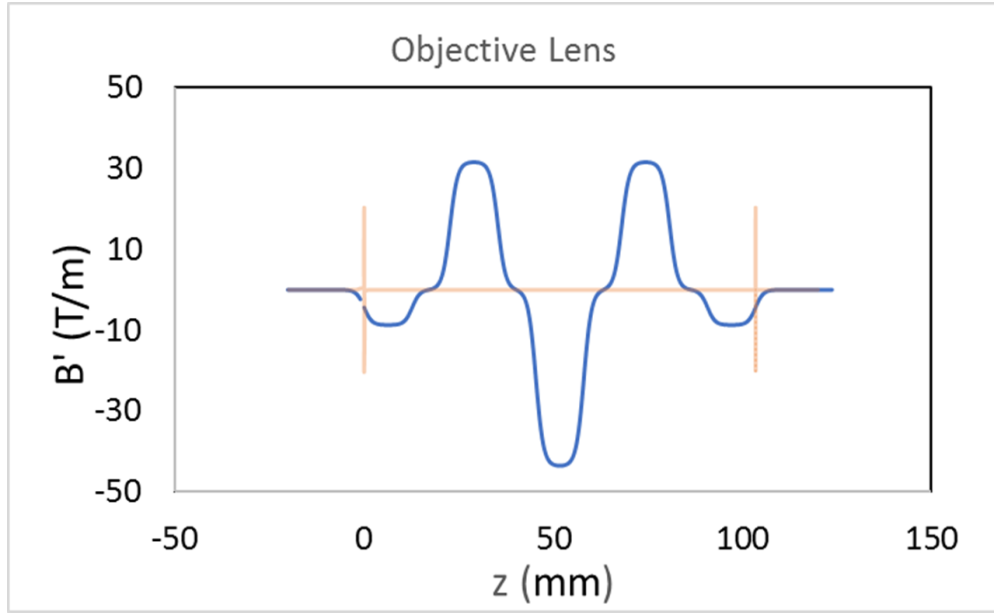


Fig. 1. The longitudinal field profile of the UEM lens.

The magnet alignment tolerances are determined by the sample plane defocus  $\Delta D = \theta_{ap}R_{12}/R_{11}$ . Here,  $R_{12}$  is the transfer matrix element, which represents the angle-to-position spread term;  $R_{11}$  is the transfer matrix element representing the magnification. The aperture angle  $\theta_{ap}$  is set to 1 mrad. The sample plane defocus is set to 1 nm for the rotation, tilt, transverse misalignment tolerances, and magnet measurement error tolerances. The sample plane defocus is set to 100 nm for the longitudinal misalignment tolerances due to the extremely tight requirement. Thanks to the design with tunable magnet-to-magnet drift spaces in each set of the lens magnets, the step size of the stepper motors moving the magnets has an adequate precision of 1  $\mu\text{m}$ .

The magnet tolerances for manufacture and measurement are specified via start-to-end simulations using COSY and GPT [4,5] codes, as shown in Table II. The errors mean to be the upper limits. The alignment tolerances are shown in Table III. We should align all the magnets to the best, especially for those magnets Q2, Q3, and Q4. Then, the adjustable drift spaces between the magnets are essential to achieve the targeted resolution.

6/13/2019 14:27		Parameter List				
The quadrupole errors in this Table are to be understood as upper limits, and the magnets to be built shall conservatively achieve these requirements.						
Line number 4 identifies the manufacturing limit.						
Line number 5 identifies the measurement error limit.						
Line #	Permanent Magnet Quadrupole Parameters					
Description	Units	Q1	Q2	Q3	Q4	Q5
1 Magnetic Length	mm	12.7	12.7	12.7	12.7	12.7
2 Aperture, min	mm	8.4	8.4	8.4	8.4	8.4
3 Field Gradient	T/m	-8.747	31.771	-43.836	31.771	-8.747
4 Integrated gradient tolerance ( $\Delta(B'L)/(B'L)$ )(deviation from design)(B=pole tip field)	%	$\pm 2$	$\pm 2$	$\pm 2$	$\pm 2$	$\pm 2$
5 Measured Integrated gradient tolerance ( $d(B'L)/(B'L)$ )(Measured error)(B=pole tip field)	%	$\pm 1.40$	$\pm 0.45$	$\pm 0.18$	$\pm 0.45$	$\pm 1.40$
6 Approx. Pole Tip Field (Reference)	T	0.0367	0.1334	0.1841	0.1334	0.0367
7 Good Field Region (diameter)	mm	5.04	5.04	5.04	5.04	5.04
8 Allowed Field Harmonic b6 @ R=2.80mm	$10^{-4}$	$\pm 1212$	$\pm 615$	$\pm 615$	$\pm 615$	$\pm 1212$
9 Allowed Field Harmonic b10 @ R=2.80mm	$10^{-4}$	$\pm 17$	$\pm 15$	$\pm 15$	$\pm 15$	$\pm 17$
10 Allowed Field Harmonic b14 @ R=2.80mm	$10^{-4}$	$\pm 6$	$\pm 3.5$	$\pm 3.5$	$\pm 3.5$	$\pm 6$

Table II Magnet tolerances include manufacture and measurement.

	Rotation						
	Q1	Q2	Q3	Q4	Q5	trim Q	SQ
Roll (mrad)	13	2.8	1.1	1.5	3.5	10.5	10.5
	Tilt						
Pitch x (mrad)	10.5	5	2.8	4	6.6	19.8	19.8
Yaw y (mrad)	10.5	4.3	4.3	3.5	6.7	20.1	20.1
<b>The longitudinal tolerance</b>							
• Sample plane defocus $\Delta D = 100\text{nm}$ . $\theta_{ap} = 1\text{mrad}$							
	Q1	Q2	Q3	Q4	Q5	trim Q	SQ
$\Delta x$ (um)	55	30	30	45	200	100	100
$\Delta y$ (um)	65	20	25	55	200	100	100
$\Delta z$ (um)	280	25	28	33	180	200	200

Table III Magnet alignment tolerances include the rotation, tit, and transverse offset

## Method and Result

### 1. Design of the UEM magnets

The permanent magnet quadrupoles (PMQ) are the building blocks of the UEM lens system, which comprises three quintuplets [6]. Each quintuplet includes five PMQs with a total number of 15 magnets. Each PMQ comprises small neodymium magnets installed in a brass magnet holder  $90^\circ$  apart to achieve a quadrupole field. The magnet assembly is populated according to the gradient strength needed. To minimize unwanted harmonics, two pairs of the  $\pm$  peaks of each PMQ are adjusted for the best matching of the field strength. Through an iterative process of measurements and adjustments, those magnets are adjusted to achieve the correct 2D

gradient. Also, a 3D measurement along the longitudinal axis at a fixed radius is made to ensure the minimum deviation from the design gradient. The deviation must not exceed the tolerance specified in Table II.

The magnet model (Fig. 2) shows a PMQ with the magnet blocks located  $90^\circ$  apart. The gaps between the opposing magnet blocks at each pole of the quadrupole are adjusted such that the 4 field peaks at  $0^\circ, 90^\circ, 180^\circ, 270^\circ$  are equal. The larger the gap (less cancellation), the stronger the field in the magnet aperture, and the higher the gradient. Configurations of the magnets with three different gradients are shown in Fig. 3: the left is for the low gradient, the middle is for the high gradient, and the right is for the medium gradient.

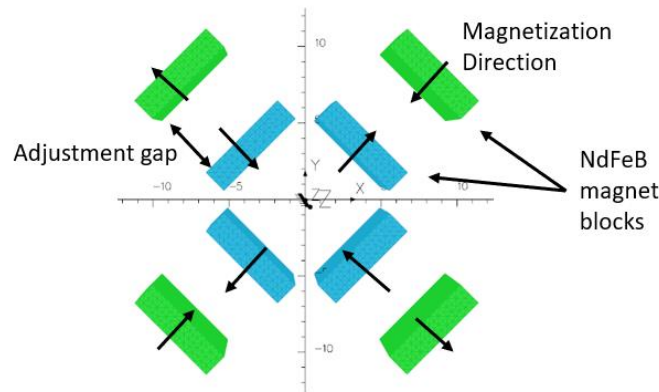


Fig. 2: Tosca model of UEM Quadrupole, showing magnetization directions.

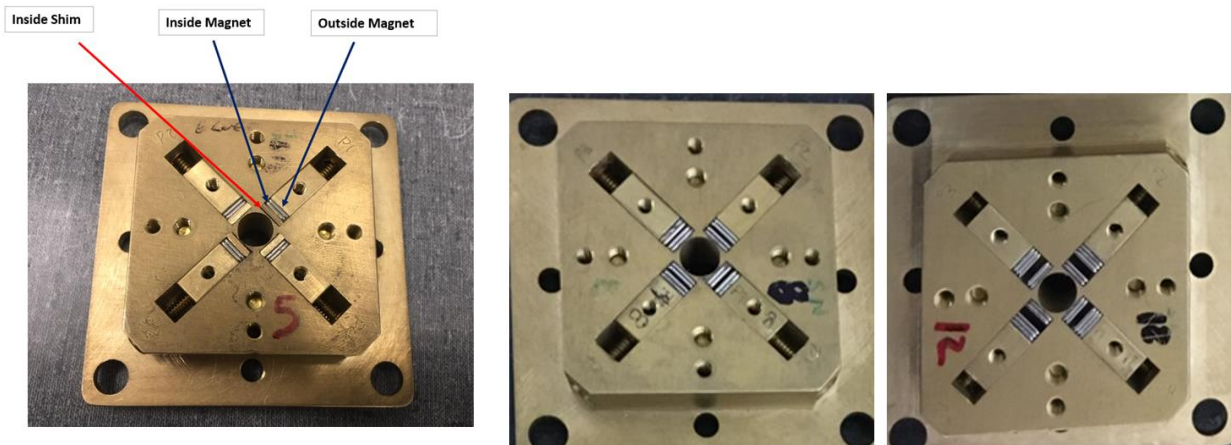


Fig. 3: (left) Low gradient magnet with inner shim and 2 magnets per pole. (middle) High gradient magnet with 2 inboard magnets and 2 outboard magnets per pole. (right) Medium gradient magnet with 2 inboard magnets and 3 outboard magnets per pole.

## 2. PMQ Measurement System

The measurements are made using a hall probe. Because of the small probe size ( $100 \times 100 \text{ mm}^2$ ), it is more practical to rotate the magnet around its magnetic center while the hall probe is

fixed at a distance ( $R > 1\text{mm}$ ) with respect to the center. The magnetic field as a function of the rotation angle is registered as the result of the rotation scan via the hall probe. Then, the harmonic analysis is performed offline using the TOSCA code [6]. The measurement system consists of a hall probe assembly and a magnet holder assembly, which are attached to a common base, as shown in Fig. 4. The details can be found in the manual of the measurement system [6].

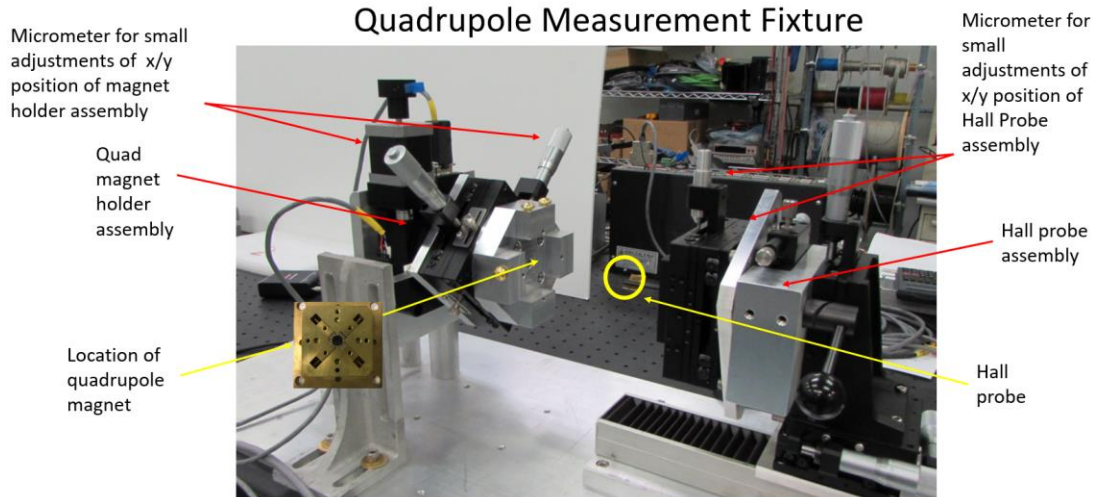


Fig. 4: Hall probe and magnet holder Assembly.

### 3. Magnetic center and rotation scan

We move the hall probe outward with reference to the magnetic center in the x-direction between P1 and P4 poles until the dial gauge reads 1.4 mm (blue dot in Fig. 5b). Then, we start the rotation scan measurement. Each scan contains 361 points, starting from  $0^\circ$  to  $360^\circ$  with a step size of  $1^\circ$ . Once the scan is complete, the measured waveform appears in the LabVIEW GUI, as shown in Fig. 6.

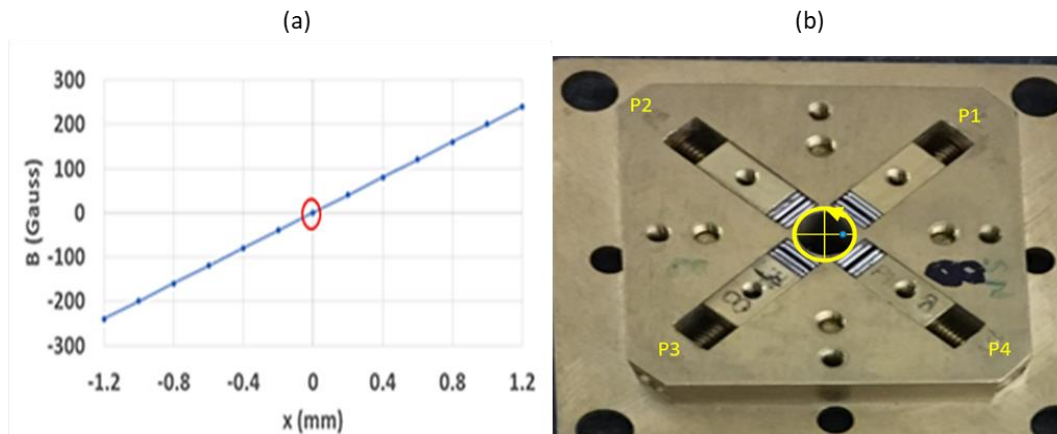


Fig. 5: (a) (left)  $B$  vs Radius. (b) (right) Rotation scan path. Hall probe position is highlighted as the blue dot.

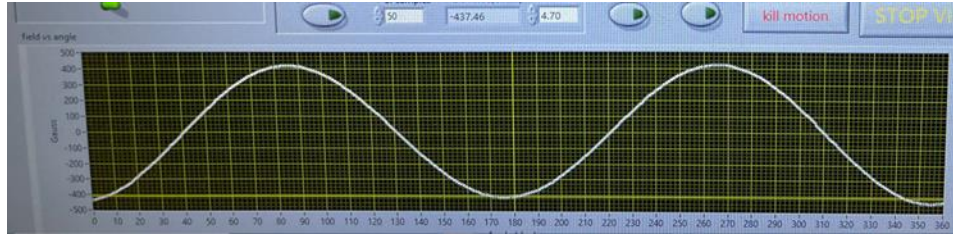


Fig. 6: The result of rotation scan: B Field (y-axis) vs angle (x-axis).

#### 4. Longitudinal scan

The longitudinal scan is done by moving the hall probe with a step size of 0.5 mm or 1.0 mm and recording the readback of the Hall probe at a fixed angle. An example of the longitudinal scan of PMQ M14 is shown in Fig. 7.

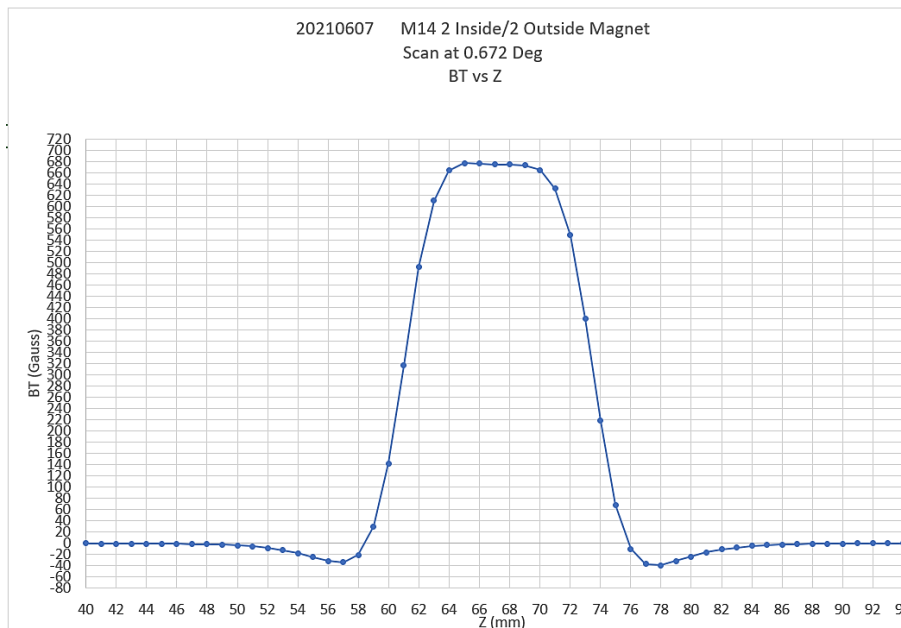


Fig. 7 The result of longitudinal scan for PMQ M14.

#### 5. PMQ misalignment

We analyze all harmonic coefficients using the result of the rotation scan. Only two harmonics,  $a_1$  and  $b_1$ , are of the top importance in determining the coordinates  $x_0$  and  $y_0$  of the magnetic center in horizontal and vertical directions, respectively. These harmonics are extracted from the rotation scan via the harmonic analysis by TOSCA model [6,7]. The detailed information is shown in Fig. 8.

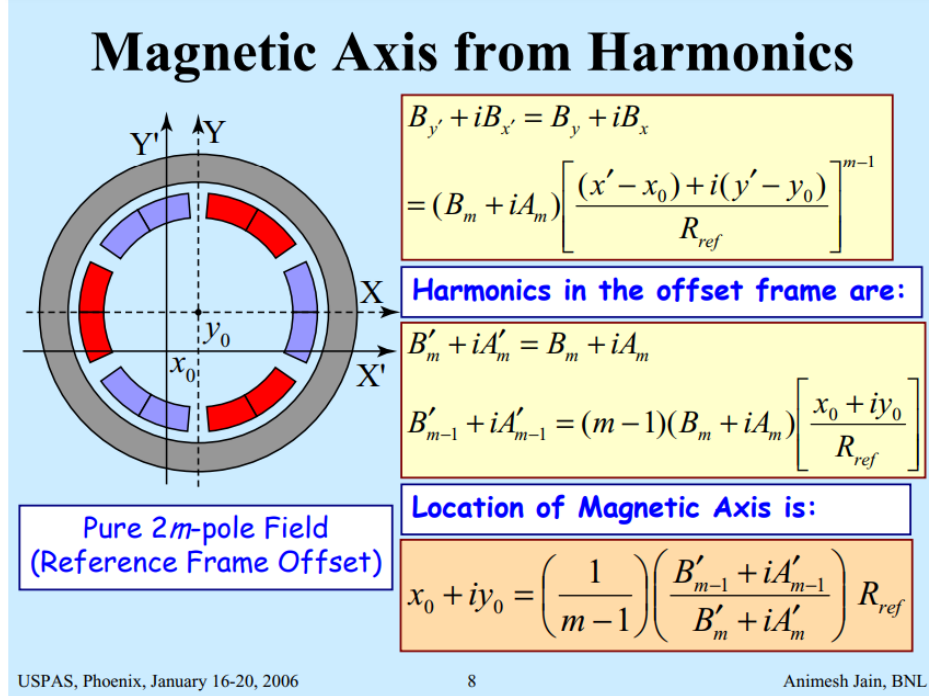


Fig. 8 Equations for extracting the transverse misalignment  $x_0$  and  $y_0$  via harmonic  $a_1$  and  $b_1$ .

### 6. Checking the measured gradient

Following the methods described before, we built all the PMQs and completed the measurements. The gradient is estimated from the results of the longitudinal scan using the formula:

$$B' = \frac{\bar{B}}{R} = \frac{\frac{1}{L} \int_{-\infty}^{+\infty} B(z, \theta_0, R) dz}{R} \quad (1)$$

To meet the measurement tolerance, we must make corrections for Eq. (1) with a scale factor. This scale factor is based on the result of the rotation scan, and it is the ratio of the fitted field amplitude  $B_{amp}$  (described later in the same section) and the field measured by the rotation scan at the position where the rotation scan and the longitude scan spatially overlap.

To extract the correct field  $B(z_0, \theta_0, R)$  for the determination of the real gradient, we must fit the rotation scan result with Eq. (2). Here, the factor  $SC_\theta$  is to correct the rotation angle  $\theta$ ;  $\theta_0$  is the offset related to  $0^\circ$  defining the angle where the rotation scan starts.  $B_{amp}$  is the corrected field amplitude.

$$B(\theta)|_{z_0, R} = B_{amp} \cdot \cos(2 \cdot SC_\theta \cdot \theta + \theta_0) + B_{offset} + BS \cdot \theta \quad (2)$$

The scale factor applied to Eq. (1) is

$$Scale \equiv \frac{B_{amp}}{B(\theta_0)|_{z_0, R}} \quad (3)$$

As an example, the measured data (blue) and the fit result (orange) for the rotation scan of PMQ M15 are shown in Fig. 9. The agreement is quite good, similar good agreements were also obtained for all PMQs.

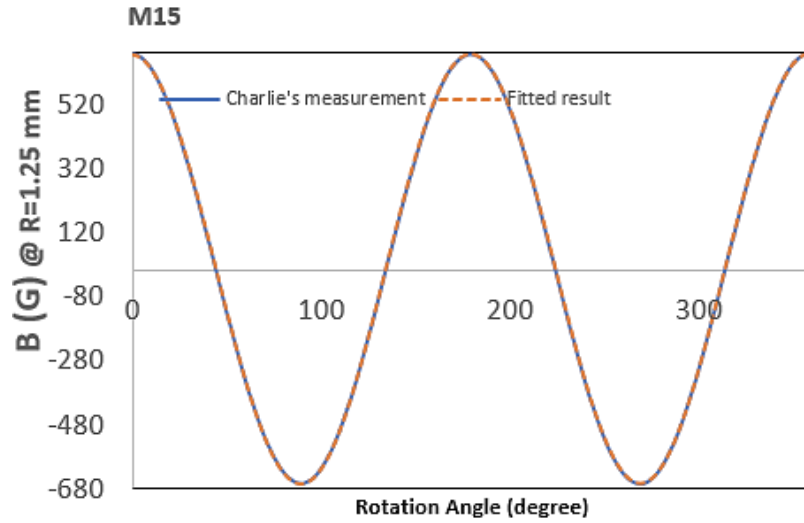


Fig. 9 The measurement (blue) and fitted result (orange) are plotted for PMQ M15.

## 7. Transverse misalignment

The misalignments extracted from the relevant harmonics have been confirmed by the TOSCA model, as shown in the correlation plots, Fig. 10.

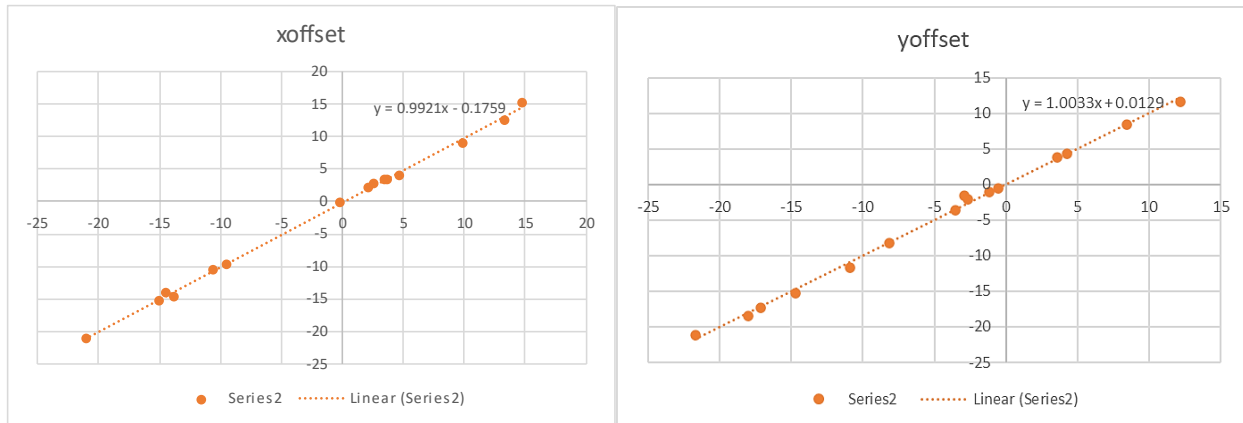


Fig. 10 Comparing the transverse misalignment in x (left) and y (right) via the harmonic method and TOSCA model.

## 8. Results of all 15 PMQs

Fig. 11 shows the results of longitudinal scans of all PMQs: low- (left), medium- (middle), and high- (right) gradient magnets. The parameters of all PMQ magnets are documented in Table IV, including the measured gradient, transverse offsets, etc.

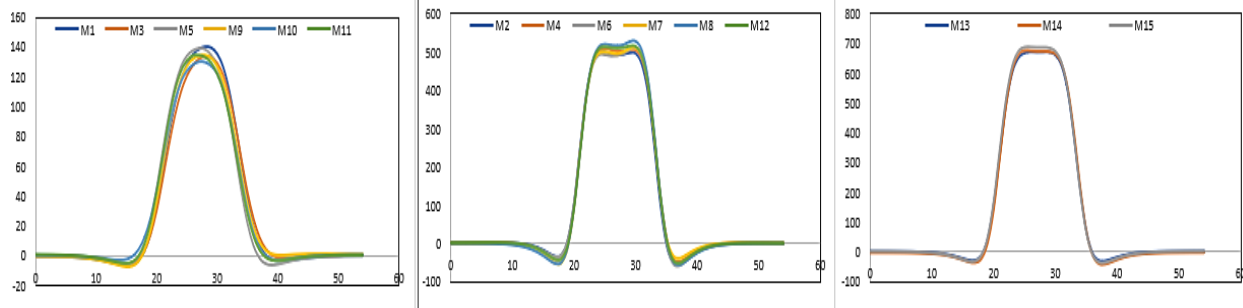


Fig. 11 Longitudinal scans of low (left), medium (middle) and high (right) gradient PMQs.

MAGNET	Quintuplet Set	Inside Shim Size (1/100 0")	# Inboard Magnets	# Outboard Magnets	B' Target Gradient (T/M)	Final B' Gradient (T/M)	Date Accepted	% Off	a1	b1	Y Offset (μm)	X Offset (μm)	Formula's xoffset	Formula's yoffset	Charlie's Toscal fit xoffset	Charlie's Toscal fit yoffset	tolerance x (um)	tolerance y (um)
M1	2	96	1	1	-8.7474	8.7835	5/26/21	0.41	-226	-156	-21.1	-14.6	-13.85037	-21.7122	-14.5548	-21.131	55	65
M3	1	96	1	1	-8.7474	8.7057	5/25/21	-0.48	124	163	11.6	15.2	14.73992	12.1738	15.2079	11.594	55	65
M5	3	96	1	1	-8.7474	8.8559	6/8/21	1.23	-11	-226	-1.0	-21.1	-21.09576	-1.17981	-21.0806	-1.03978	55	65
M9	2	96	1	1	-8.7474	8.8082	6/3/21	0.69	-198	-150	-18.5	-14.0	-14.49007	-18.0401	-13.995	-18.513	55	65
M10	3	96	1	1	-8.7474	8.75	6/10/21	0.03	-164	134	-15.3	12.5	13.24803	-14.7074	12.5022	-15.334	55	65
M11	1	96	1	1	-8.7474	8.7216	5/26/21	-0.30	46	-2	4.3	-0.2	-0.272722	4.25621	-0.1866	4.301	55	65
M2	3	0	2	3	31.771	31.7192	4/22/21	-0.16	125	-96	11.7	-9.0	9.902503	-10.9255	8.9568	11.6875	30	20
M4	3	0	2	3	31.771	31.66	4/15/21	-0.36	17	164	1.6	15.3	-15.07011	-2.92018	-15.3012	1.5895	30	20
M6	1	0	2	3	31.771	31.5939	4/23/21	-0.56	22	104	2.1	9.7	-9.528333	-2.64998	-9.7032	2.057	30	20
M7	2	0	2	3	31.771	31.7274	6/7/21	-0.14	39	-36	3.6	-3.4	3.491966	-3.51162	3.3588	3.6465	30	20
M8	2	0	2	3	31.771	31.8628	5/5/21	0.29	185	-44	17.3	-4.1	4.608651	-17.142	4.1052	17.2975	30	20
M12	1	0	2	3	31.771	31.7868	4/29/21	0.05	-40	113	-3.7	10.6	-10.61292	3.5736	-10.5429	-3.74	30	20
M13	1	0	2	2	-43.836	43.8394	5/4/21	0.01	-88	37	-8.2	3.5	3.676675	-8.14549	3.4521	-8.228	30	25
M14	3	0	2	2	-43.836	43.9321	6/7/21	0.22	-6	23	-0.6	2.1	2.124688	-0.52676	2.11128	-0.57043	30	25
M15	2	0	2	2	-43.836	43.8603	5/13/21	0.06	90	29	8.4	2.7	2.561912	8.46374	2.7057	8.415	30	25

TABLE IV Information of all the PMQ magnets, including the measured gradient and transverse offsets.

## Conclusion

All the PMQs have been measured and meet the specification. Three quintuplets include a total number of fifteen PMQs (Table IV). Those PMQs were installed in the UEM beamline as the Objective, Projector 1, and Projector 2 lenses. The selection rules for each lens are to choose PMQs with the closest matched gradients and minimum harmonic components to build those lenses with the order of Objective, Projector 1, and Projector 2. This is because the Objective lens is the most important part of the system, it determines the ultimate spatial resolution. Now, the UEM instrument is ready for beam commissioning, which is to be scheduled when the acceptable beam quality is achieved by the UED electron source at ATF.

## References

- [1] Preliminary Design Review Ultrafast Electron Microscope Report. D. Zakharov (BNL), M. Marko (Wadsworth), Q. Liu (BNL), M. Fedurin (BNL), E. Wang (BNL) and P. Musumeci (UCLA) (Chair).
- [2] Preliminary Design Review Talk "Demonstration of feasibility of sub-nm, picosecond electron microscope for the life sciences – Physics". X. Yang and UEM team.

- [3] Design of compact ultrafast microscopes for single- and multi-shot imaging with MeV electrons. *Ultramicroscopy*. 194 143-153 (2018).  
Wan, W., Chen, F. & Zhu, Y.
- [4] General Particle Tracer (GPT) code. <http://www.pulsar.nl/gpt>.
- [5] Start-to-end self-consistent simulation of the UEM beamline. NSLSII technote xxx (2020).
- [6] Test Procedure of UEM Quad Measurement, C. Spataro, NSLS-II Mechanical Engineering Group.
- [7] Determination of Magnetic Axis, Animesh Jain, US Particle Accelerator School, Phoenix, Arizona, January 16-20, 2006